Anomaly Detection for Industrial Inspection using Convolutional Autoencoder and Deep Feature-based One-class Classification

Jamal Saeedi[a] and Alessandro Giusti[b]
Dalle Molle Institute for Artificial Intelligence (IDSIA USI-SUPSI), Lugano, Switzerland

Keywords: Anomaly Detection, Industrial Inspection, Convolutional Autoencoder, Deep Feature Embedding, One-Class classification.

Abstract: Part-to-part and image-to-image variability pose a great challenge to automatic anomaly detection systems; an additional challenge is applying deep learning methods on high-resolution images. Motivated by these challenges together with the promising results of transfer learning for anomaly detection, this paper presents a new approach combing the autoencoder-based method with one class deep feature classification. Specifically, after training an autoencoder using only normal images, we compute error images or anomaly maps between input and reconstructed images from the autoencoder. Then, we embed these anomaly maps using a pre-trained convolutional neural network feature extractor. Having the embeddings from the anomaly maps of training samples, we train a one-class classifier, k nearest neighbor, to compute an anomaly score for an unseen sample. Finally, a simple threshold-based criterion is used to determine if the unseen sample is anomalous or not. We compare the proposed algorithm with state-of-the-art methods on multiple challenging datasets: one representing zipper cursors, acquired specifically for this work; and eight belonging to the recently introduced MVTec dataset collection, representing various industrial anomaly detection tasks. We find that the proposed approach outperforms alternatives in all cases, and we achieve the average precision score of 94.77% and 96.35% for zipper cursors and MVTec datasets on average, respectively.

1 INTRODUCTION

Anomaly detection (AD) can be defined as the identification of items or events that do not comply with an expected pattern or to other items in a dataset.

For visual inspection tasks in the manufacturing industry, often there are a few examples of defective samples or it is unclear what kinds of defects may appear. Therefore, it is a challenge to provide a large enough dataset in which each sample is labeled as either "normal" or "abnormal", as it is needed for traditional supervised classification techniques (Saeedi et al., 2021). Many relevant applications must rely on semi-supervised algorithms for identifying anomalous samples. Semi-supervised techniques construct a model given only normal training samples representing normal behavior and then test the unseen sample by the learned model.

The objective of the project presented in this paper is to automate the inspection process of zipper cursors in the production lines using an image acquisition system (IAS) and dedicated software based on the semi-supervised pipeline. Here, we assume that the object for inspection has a rigid shape and we use a reference image for image registration and alignment as a pre-processing step.

With the recent advances in deep neural networks, reconstruction-based methods deploying autoencoder (AE) have shown great potential for AD tasks. These methods assume that normal and anomalous samples could lead to significantly different embeddings and therefore the corresponding reconstruction errors can be used to distinguish normal and anomalous samples (Jinwon and Sungzoon, 2019; Kingma and Welling, 2014). An AE is a neural network that is trained to learn reconstructions that are close to its original input.

The state-of-the-art methods based on deep learning applying AE and its variations (Chao-Qing et al., 2019), mostly considering public data-set with

[a] https://orcid.org/0000-0002-3143-8107
[b] https://orcid.org/0000-0003-1240-0768

Saeedi, J. and Giusti, A.
Anomaly Detection for Industrial Inspection using Convolutional Autoencoder and Deep Feature-based One-class Classification.
DOI: 10.5220/0010780200003124
In *Proceedings of the 17th International Joint Conference on Computer Vision, Imaging and Computer Graphics Theory and Applications (VISIGRAPP 2022) - Volume 5: VISAPP*, pages 85-96
ISBN: 978-989-758-555-5; ISSN: 2184-4321

small dimensions for evaluation, e.g. MNIST (LeCun, 1998) (28×28), Fashion-MNIST (Xiao et al., 2017) (28×28), CIFAR-10 (Krizhevsky and Hinton, 2009) (32×32), ImageNet (Deng et al., 2009) (224×224). However, the image dimension is rather high in industrial inspection scenarios, e.g. MVTec dataset (Bergmann et al., 2019a) (1024 ×1024). Designing a proper AE with high-resolution images results in a large network size. Training such a large network is very time-consuming and there is a risk of network overfitting due to the small number of training samples in some cases.

Downsizing (Bergmann et al., 2019a), and patch-wise inspection (Matsubara et al., 2018) are the two pre-processing methods that have been applied to address the size issue in the past, while both approaches could be problematic for AD. In some cases, the defect or anomaly is very small that could be lost after downsizing. In addition, by applying patches for inspection, we could miss defects that are larger than the patch size. In this paper, we proposed a new framework based on conditional patch-based convolutional autoencoder (CPCAE) to address the size issue. The proposed method applies both downsizing and patch extraction to avoid the aforementioned problems. Specifically, overlapping patches are extracted from downsized images to train the AE. Together with the patches, we give the network the index of the patches in the image (i.e. the patches' location) as an auxiliary input. In this way, each patch remembers where it is coming from in the image. The idea comes from the recently developed conditional variational autoencoder (VAE) (Pol et al., 2019), in which the method was used for MNIST data AD, and class labels (from 0 to 9) were considered as a condition for training the VAE. For anomaly map and score calculation for a test image, the procedure is to apply the reverse of patch extraction and upsizing for the AE's output. The anomaly map is then obtained using the difference of the input and reconstructed images.

The AE-based methods detect anomalies by comparing the input image to its reconstruction in pixel space. This can result in poor AD performance due to simple per-pixel comparisons and imperfect reconstructions (Bergmann et al., 2019b, Nalisnick et al., 2018). In this study, we have proposed a new approach to incorporate transfer learning with the AE-based AD method to avoid computing anomaly scores using AE's reconstruction error. Specifically, we apply a one-class classifier to the anomaly maps generated by AE to compute anomaly scores. One-class classification using deep feature extracted from a pre-trained convolutional neural network (CNN) is a new trend in recent years for AD (Perera and Patel, 2019; Oza and Patel, 2019; Bergman et al., 2020), which suggest that these feature spaces generalize well for AD task and even simple baselines outperform deep learning approaches (Kornblith et al., 2019).

Motivated by the challenges mentioned for AD in industrial inspection, shortcomings related to AE-based method together with promising results with transfer learning reported in recent works (Perera and Patel, 2019; Oza and Patel, 2019; Ruff et al., 2018; Bergman et al., 2020; Burlina et al., 2019), this paper presents a new framework combining AE-based method with one class deep feature classification. Specifically, instead of computing anomaly scores from anomaly maps obtained from a trained AE, we embed the anomaly maps using a pre-trained CNN (on Imagenet dataset) feature extractor. Having the embedding from the anomaly maps of training samples, we train a one-class classifier, e.g. k nearest neighbor (k-NN) to compute anomaly score for unseen samples. In this way, we leverage transfer learning together with AE using a hybrid framework to avoid problems due to simple per-pixel comparisons or imperfect reconstructions of the AE-based method.

We evaluate the proposed method extensively on different datasets, including the zipper cursor dataset, which has been acquired and introduced specifically for this study, and a recently introduced MVTec AD dataset which involves different types of industrial inspection (Bergmann et al., 2019a). We show that AE outperforms the state-of-the-art techniques when combined with one-class deep feature classification using the proposed framework.

Our main contributions are summarized as follows:

- We propose a novel concept using CPCAE for AD to tackle the challenges related to the high-resolution images in industrial inspection scenarios.
- We propose a hybrid framework based on transfer learning to calculate anomaly scores instead of AE's reconstruction error. This new method embeds anomaly maps computed by AE using a pre-trained CNN feature extractor to train a one-class classifier.
- We demonstrate state-of-the-art performance on different datasets including zipper cursor and MVTec anomaly detection datasets.

The remainder of this paper is organized as follows. After a review of related work in Section 2, the proposed method based on CPCAE and transfer learning is discussed in Section 3. Section 4 demonstrates experimental results and discussion. Finally, the conclusions and future works are given in Section 5.

2 RELATED WORK

AD methods can be broadly categorized into probabilistic, proximity-based, boundary-based, reconstruction-based, and hybrid approaches, which are shortly discussed in the following:

Probabilistic approaches, such as Gaussian mixture models (Eskin, 2000) and kernel density estimation (Xu et al., 2012) assume that the normal data follow some statistical model. During the training, a distribution function is being fitted on the features extracted from the normal samples. Then, during the test, those samples which are mapped to different statistical representations are considered anomalous (Kingma and Welling, 2014).

Proximity-based algorithms assume that the proximity of an anomalous object to its nearest neighbors significantly deviates from its proximity to most of the other objects in the dataset. Given a set of objects in feature space, a distance measure can be used to compute the similarity between objects, and then objects that are far from others can be regarded as anomalies. These methods depend on the well-defined similarity measure between two data points. The basic proximity-based methods are the local outlier factor (Breunig et al., 2000) and its variants (Tang and He, 2017).

Boundary-based approaches, mainly involving one-class support vector machines (SVM) (Scholkopf et al., 2001) and support vector data description (SVDD) (Tax et al., 2004), usually try to define a boundary around the normal samples. Anomaly sample is determined by their location to the boundary. A recent trend in the boundary-based AD methods is to utilize transfer learning techniques using a pre-trained CNN network to extract discriminative embedding vectors for classification (Burlina et al., 2019; Andrews et al, 2016; Nazaré et al., 2018; Napoletano et al., 2018)

Reconstruction-based approaches assume that anomalies cannot be compressed and therefore cannot be efficiently reconstructed from their low dimensional embeddings. In this category, principal component analysis (Olive, 2017) and its variations (Harrou et al., 2015; Baklouti et al., 2016) are widely used. Besides, AE and VAE based methods also belong to this category (Jinwon and Sungzoon, 2019; Kingma and Welling, 2014).

Hybrid approaches utilize both reconstruction and classification-based methods in a hybrid framework. Specifically, these methods use AE to generate feature embedding for training a one-class classifier in which the latent space variables act as the embedding. Kawachi et al. (2018) proposed an assumption that the anomaly prior distribution is a complementary set of the prior distribution of normal samples in latent space. Based on this assumption, the anomalous and the normal data have complementary distributions which means that they can be separated in the latent space, then it is possible to apply a one-class classifier to detect anomalies. Similarly, Guo et al. (2018) used the compressed hidden layer vector of a trained AE on normal data to train a k-NN for AD.

In this paper, we aim to propose a better discriminative embedding as compared to the AE's latent space variables for one-class classification. The proposed method presented in this paper can be considered as a hybrid approach as we utilize both AE and classification-based approaches, which is fully discussed in the next section.

3 PROPOSED METHOD

This section describes the core principles of our proposed CPCAE method which is shown in Figure 1. We operate in a semi-supervised setup, where examples of anomalous instances are not available. Therefore, we train a model using only normal samples which are initially registered and aligned. The proposed method consists of two parts including anomaly map generation using AE and anomaly score calculation using deep feature one class classification as shown in Figure 1. Using this hybrid framework, we deploy both AE as well as transfer learning combined with one class classification to improve the AD results as compared to each method individually.

In the following sub-sections, we discuss the proposed CPCAE method, and deep feature one-class classification.

3.1 Conditional Patch-based Convolutional Autoencoder

Autoencoders attempt to reconstruct an input image $x \in \mathbb{R}^{C\times H\times W}$ through a bottleneck, mapping the input image into a lower-dimensional space which is called the latent space (Chao-Qing et al., 2019; Bergmann et al., 2019b). An AE consists of an encoder, $E : \mathbb{R}^{C\times H\times W} \rightarrow \mathbb{R}^{d}$, and a decoder, $D : \mathbb{R}^{d} \rightarrow \mathbb{R}^{C\times H\times W}$, where d indicates the latent space's

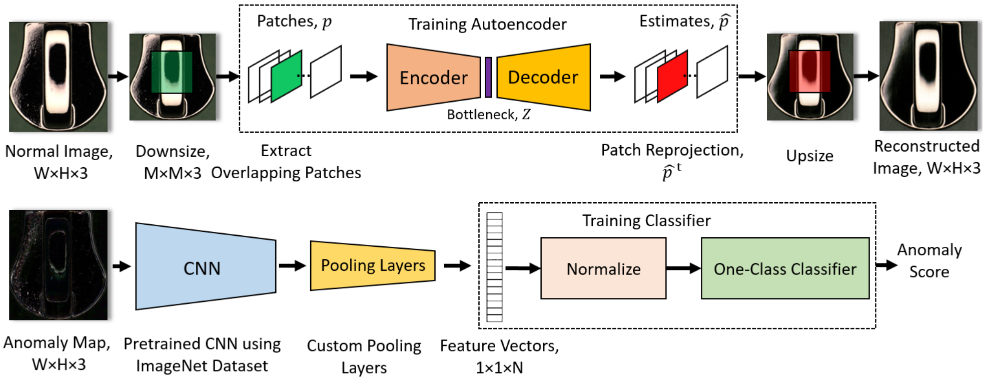

Figure 1: Block diagram of the proposed anomaly detection method (dashed lines show the steps involved in the training step).

dimensionality and C, H, W represent the channels, height, and width of the input image, respectively. The overall process can be written as follows:

$$\hat{x} = D\big(E(x)\big) = D(z) \qquad (1)$$

where z is the latent vector and $\hat{x}$ the reconstruction of the input. The functions E and D are parameterized by CNNs.

For simplicity and computational speed, a per-pixel error measure such as the L_2 loss is chosen to force the AE to reconstruct its input:

$$L_2(\mathrm{x}, \hat{x}) = \sum_{c=0}^{C}\sum_{h=0}^{H}\sum_{w=0}^{W}\big(\mathrm{x}(c,h,w) - \hat{x}(c,h,w)\big)^2 \qquad (2)$$

where $\mathrm{x}(c,h,w)$ denotes the intensity value of image x at the pixel (c,h,w). During evaluation, the per-pixel ℓ^2-distance of x and $\hat{x}$ is compute to obtain a residual map $\mathrm{R}(\mathrm{x},\hat{x}) \in \mathbb{R}^{\mathrm{C}\times\mathrm{H}\times\mathrm{W}}$.

For the AD task, AE is only trained on defect-free samples. During the test, the AE is failed to reconstruct defects that have not been seen during the training. The reconstruction error, L_2, of each test data is then regarded as the anomaly score. Finally, the data with a high anomaly score is defined as anomalies.

There are two main issues for deploying AE for the AD task in an industrial inspection scenario including the high-resolution images and poor performance due to simple per-pixel comparisons and imperfect reconstructions (Bergmann et al., 2019b; Nalisnick et al., 2018). In this paper, we address the high resolution image issue by applying overlapping patches along with conditional learning for AE, which is discussed in this sub-section. In addition, we propose a new approach to incorporate transfer learning with the AE to avoid computing anomaly scores using simple per-pixel comparisons, which is discussed in the next sub-section.

We use downsizing and patch extraction to resolve the high-resolution image problem for AE modeling. It is assumed here that by downsizing the input image to some extent, its normality (i.e. the image details that represent normal class) are preserved. After downsizing the input image, overlapping patches are extracted to train the AE. Together with the patches, the number of the patches in the image (i.e. the patches' location) is given to the network as a conditional variable. The idea is to feed both local (patches) and global (conditions) information at the same time to the AE. The conditional variables help the AE network to train more efficiently and also to avoid reproducing small defects given a defective test image to the network. For anomaly map calculation given a test image, the procedure is to apply the patch reprojection and upsizing of the AE's output. The anomaly map is then obtained using the difference of the input and reconstructed image.

The most common architecture utilized for AE in AD is the convolutional layers followed by the pooling layers and the fully connected layers in the encoder side, and fully connected layers followed by the convolutional layers and up-sampling in the decoder side (Ribeiro et al., 2018). It is not recommended to use convolutional layers without dense layers for the AD task, because this type of network is able to memorize the spatial information of input and is somehow able to reconstruct the defects given the test image. AE deploying only convolutional layers fits better for other applications like image segmentation and compression in which detailed spatial information is very important for encoding (Badrinarayanan et al., 2017; Yildirim et al., 2018).

The proposed architecture for CPCAE is shown in Figure 2. We utilize convolutional layers with the stride in the encoder side and convolutional transpose layers with the stride on the decoder side. The convolutional (transpose) layers with the stride allow the network to learn spatial subsampling (up-sampling) from data, leading to a higher capacity of transformation. In addition, we use concatenation in the encoder part of AE to incorporate the new conditional variable (the index of the patches, i.e. patches' number divided by total number of patches) into our model. Similarly, the decoder is also concatenated with the conditional vector.

The proposed CPCAE generates anomaly maps to be used for training a one-class classifier in the second step of the proposed hybrid method. The challenge here is how to train the one-class classifier using the training set already applied for the AE training. One way to address this issue is to split the training set into two parts to be separately used for each step. However, since the training set in some cases including the current project is too small, splitting would decrease AE's capability to learn normal behavior. Another way is to train an AE using sparse information of the training set to avoid network overfitting and to preserve enough information in anomaly maps for the classifier training.

For a sparse autoencoder, in most cases, the loss function is constructed by penalizing activations of hidden layers so that only a few nodes can activate when a single sample is fed into the network. L_1 and L_2 regularizations are widely used in deep learning, and the main difference between them is that L_1 regularization tends to reduce the penalty coefficients to zero, while L_2 regularization would move coefficients near zero. More details can be reached here (Chang et al., 2019). The loss function using L_1 regularization is selected here as follows:

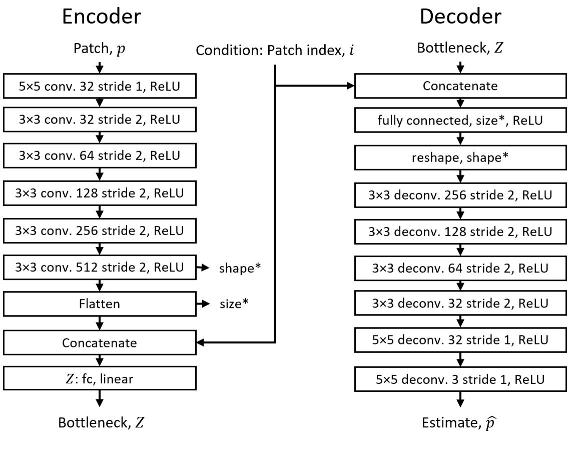
Encoder
Decoder
Patch, p
Condition: Patch index, i
Bottleneck, Z
5×5 conv. 32 stride 1, ReLU
3×3 conv. 32 stride 2, ReLU
3×3 conv. 64 stride 2, ReLU
3×3 conv. 128 stride 2, ReLU
3×3 conv. 256 stride 2, ReLU
3×3 conv. 512 stride 2, ReLU
shape*
Flatten
size*
Concatenate
Z: fc, linear
Bottleneck, Z
Concatenate
fully connected, size*, ReLU
reshape, shape*
3×3 deconv. 256 stride 2, ReLU
3×3 deconv. 128 stride 2, ReLU
3×3 deconv. 64 stride 2, ReLU
3×3 deconv. 32 stride 2, ReLU
5×5 deconv. 32 stride 1, ReLU
5×5 deconv. 3 stride 1, ReLU
Estimate, $\hat{p}$

Figure 2: The architecture of proposed CPCAE for anomaly map generation.

$$Loss = L_2(\mathrm{x}, \hat{x}) + \lambda \sum_i \left|a_i^{(h)}\right| \tag{3}$$

the second term penalizes the absolute value of the vector of activations a in layer h for sample i. A hyperparameter λ is also used to control its effect on the whole loss function.

3.2 Deep Feature-based One-class Classification

In this sub-section, the second step of the proposed method which involves feature extraction using a pre-trained CNN model followed by a one class classifier is explained. Specifically, the anomaly maps generated using AE in the first step, are used to train a one class classifier as shown in Figure 1. Using the binary classification on top of the AE result, we would like to leverage the transfer learning through feature extraction via a pre-trained CNN network and to avoid computing anomaly scores using simple per-pixel comparisons of AE. The performance of many supervised computer vision algorithms is improved by transfer learning (Kornblith et al., 2019; Burlina et al., 2019), i.e. by using discriminative embeddings from the pre-trained networks. This is also true for semi-supervised AD tasks as recent works suggest that these feature spaces together with a one class classifier outperform AE-based approaches (Nazaré et al., 2018).

The second step of the proposed AD method takes a set of anomaly maps generated by AE, $X_{train} = x_1, x_2 \dots x_N$. It uses a pre-trained feature extractor pre-trained on the Imagenet dataset, F to extract features from the entire training set, $f_i = F(x_i)$. The training set is now summarized as a set of embeddings $F_{train} = f_1, f_2 \dots f_N$. The choice of deep network and its depth are data-related and should be selected experimentally. In this study, we use Xception network just before the global pooling layer (Chollet, 2017). Xception can be considered as an extreme Inception architecture (Szegedy et al., 2016), which introduces the idea of depthwise separable convolution. More mathematical details can be reached here (Chollet, 2017). The global max pooling layer is usually used on top of the last convolutional layer of pre-trained networks to generate feature embedding (Nazaré et al., 2018). Here, we apply a new pooling layer to generate final image embedding as shown in Figure 3. Since we feed the input image

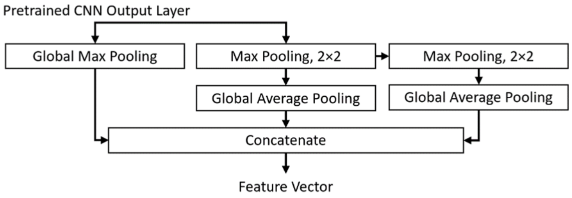

Figure 3: Proposed pooling layer used on top of the pre-trained CNN network for feature extraction.

without downsizing into the pre- trained network, the number of features after a global max-pooling layer are very small to represent a high-resolution image. Using the new pooling layer which consists of parallel and cascade pollings along with concatenation, we have three times more features as compared to the traditional way to generate final embedding.

Having the image embedding after normalization (mean removal and variance scaling), a suitable one-class classifier such as one-class SVM (Scholkopf et al., 2001), SVDD (Tax et al., 2004), or k-NN (Bergman et al., 2020), can be trained on the embeddings. In this study, k-NN is chosen as the classifier which is widely applied for AD tasks (Bergman et al., 2020; Nazaré et al., 2018; Guo et al., 2018). The advantage of k-NN-based approaches is that they do not need an assumption for the data distribution and can be applied to different data types.

To detect if a new sample y is anomalous, we first extract its feature embedding using (7) and normalize it. We then compute its k-NN distance and use it as the anomaly score as follows:

$$d(y) = \frac{1}{k} \sum_{f \in N_k(f_y)} \left\| f - f_y \right\|^2 \tag{4}$$

$N_{\mathrm{k}}(f_y)$ denotes the k nearest embeddings to f_y in the training set F_{train}. Euclidean distance is used here that often achieves superior results on features extracted by deep networks (Bergman et al., 2020), but other distance measures can be similarly used. We determine if an image y is normal or anomalous by confirming if the distance $d(y)$ is larger than a threshold.

4 EXPERIMENTAL RESULTS AND DISCUSSION

In this Section, the results of the proposed method for the AD task is presented. In addition, it is discussed how to collect data for zipper cursors and evaluate the proposed framework as well as several state-of-the-art approaches. In the following sub-sections, we discuss the following: experimental setup, dataset, evaluation metrics, evaluated methods, and AD results.

4.1 Experimental Setup

The IAS used here is a CV-X series vision system from KEYENCE, which is a multi-modes IAS. The model for the camera, lens, and lighting system are as follows: CA-H200MX, CA-LHR50, and CA-DRM10X. We use a 2-megapixel camera that generates images with 1600×1200 size. In the current IAS system setup, we use a diffused ring light system near to the object in which the object is illuminated from a low angle by uniform diffuse light through the light conduction plate. The IAS together with the camera and lighting stand with fixture and holder is shown in Figure 4.

4.2 Dataset

The zipper cursor dataset including six different types selected here is summarized in Table 1. The anomalies manifest themselves in the form of bubble, residue, halo, and scratches. In addition to zipper cursor dataset, we evaluate the proposed method on the MVTec dataset (Bergmann et al., 2019a). The MVTec dataset comprises 15 categories, however, we only consider 8 of 15 categories, which have rigid shapes that can be registered. Table 2 gives an overview of each object’s category. The anomalies consist of different types of defects such as scratches, dents, contaminations, and various structural changes. For all datasets, pixel values of all images are normalized to [0, 1], and the images are cropped to maximize the field of view. Figure 5 shows different sets of zipper cursors and different categories of MVTec datasets used for the analysis.

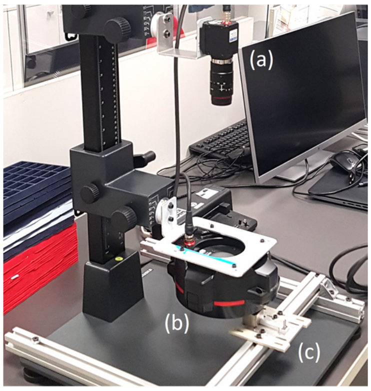

Figure 4: Image acquisition setup, (a) CV-X series vision system from KEYENCE, (b) Lighting system, and (c) Holder and fixture.

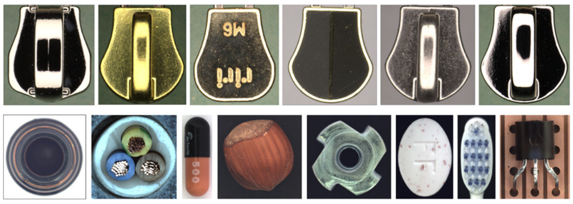

Figure 5: Anomaly detection dataset, first row, left to right: zipper cursor dataset sets. #1 to #6. bottom row, left to right: "Bottle", "Cable", "Capsule", "Hazelnut", "Metal Nut", "Pill", "Toothbrush", and "Transistor".

Table 1: Statistical overview of the zipper cursor dataset.

Set	# Train	# Test (normal)	# Test (defective)
# 1	60	55	148
# 2	60	47	84
# 3	49	33	14
# 4	40	39	36
# 5	44	19	31
# 6	28	23	18

Table 2: Statistical overview of the MVTec AD dataset.

Set	# Train	# Test (normal)	# Test (defective)
Bottle	209	20	63
Cable	224	58	92
Capsule	219	23	109
Hazelnut	391	40	70
Metal Nut	220	22	93
Pill	267	26	141
Toothbrush	60	12	30
Transistor	213	60	40

4.3 Evaluation Metrics

Receiver operator characteristic (ROC) and precision-recall (PR) curves are common metrics for AD tasks which are defined over all possible decision thresholds. It is also useful to quantitatively evaluate the model performance using a single value rather than comparing curves. The area under the ROC curve (AUC) and average precision (AP) are the common metrics that are obtained using ROC and PR curves, respectively. AP summarizes a PR curve by a sum of precisions at each threshold, multiplied by the increase in recall, which is an approximation of the area under the PR curve. Since AD task always has a large skew in the class distribution, AP gives a more accurate assessment of an algorithm's performance (Davis and Goadrich, 2006). In our experiments, ROC curve, AUC, and AP were used to evaluate the performance.

4.4 Evaluated Methods

We compare the proposed AD method with four different approaches including AE (Bergmann et al., 2019a), deep feature one class classifier (Perera and Patel, 2019), variation (Steger et al., 2018) and nearest neighbor (NN) approaches (Vaikundam et al, 2016). For the evaluation of the AE method, we use the same AE architecture described in the paper for the proposed method. For deep feature one classifier, we use the implementation proposed in (Perera and Patel, 2019), which applied a pre-trained CNN network to the image and extract features using global max pooling. After normalization, k-NN is used to generate anomaly scores ($k = 15$ is used for classifier). The variation is a baseline method, which is based on statistics, mean and standard deviation, computed from the normal training set. Anomaly maps are then obtained by computing the distance of each test pixel's gray value to the computed pixel mean relative to the computed standard deviation. The anomaly score is obtained using the sum of squares of pixels in the anomaly map. NN is another baseline method in which the anomaly score is obtained by computing the distance (usually l_2) between the test sample and its most similar image inside the normal training set. It should be mentioned that parameters tuning is performed for different models included in the comparison to find the best solution for them. Apart from the methods that have been implemented for comparison, we also report AUC results for the MVTec dataset from recently published deep-learning-based methods consisting of GeoTrans (Golan et al., 2018), GANomaly (Akcay et al., 2018), VAE (Jinwon and Sungzoon, 2019), AnoGAN (Schlegl et al., 2017), and AE applying structural similarity index measure (SSIM) (Bergmann et al., 2019b), taken directly from (Chao-Qing et al., 2019) and (Bergmann et al., 2020).

4.5 Anomaly Detection Results

The first experiment is the two-dimensional tSNE visualizations of the extracted features from the anomaly maps as compared to the AE's latent space variables for normal and anomalous images in the test set (Van der Maaten and Hinton, 2008). AE's latent space variables are also being used as image embedding for AD in recent years (Kawachi et al., 2018; Guo et al., 2018; Amarbayasgalan et al., 2018). The tSNE visualizations are shown in Figure 6 for zipper cursor and MVTec datasets. Qualitatively, features extracted by the proposed method facilitate better distinction between normal and anomalous images as compared to the AE's latent space variables.

The second experiment presents the AD results of the proposed method as well as the baselines and deep-learning based approaches for zipper cursors and MVTec datasets. Tables 3 and 4 show AUC and AP metrics, and Figures 7 and 8 show the ROC curves. It can be seen from the results that the proposed hybrid framework outperformed state-of-the-art methods in terms of different metrics, specifically PR, which gives a more accurate picture of an algorithm's performance when there is a large skew in the class distribution (Davis and Goadrich, 2006). The second best method on average is AE for the zipper cursor dataset and deep feature classification for the MVTec dataset. This is because AE is able to generalize better on the zipper cursor dataset which has simpler appearances as compared to the MVTec dataset. The baseline approaches including variation and NN methods could not produce reliable results. In addition, the proposed method outperformed recently published deep learning-based methods in terms of AUC metric for the MVTec dataset as shown in Table 4.

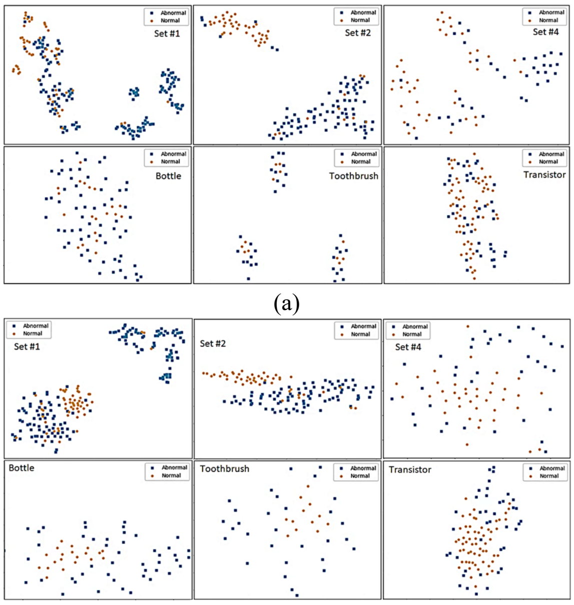

(a)

(b)

Figure 6: 2D t-SNE plots of the feature embedding obtained using (a) the AE's latent space representation and (b) proposed embedding for different datasets, which are mentioned in the corner of each plot.

Table 3: Anomaly detection results for the zipper cursor dataset.

Methods	Metrics	Set #1	Set #2	Set #3	Set #4	Set #5	Set #6	Mean
Proposed	AUC	95.67	96.90	95.20	88.08	94.64	96.10	**94.43**
	AP	98.35	98.16	90.90	88.81	96.00	96.43	**94.77**
AE (L_2)	AUC	87.81	95.59	92.21	77.54	78.48	91.11	87.12
	AP	95.24	97.05	87.88	83.01	82.47	90.17	89.30
Deep Feature	AUC	85.32	95.77	80.81	74.97	62.15	93.77	82.13
	AP	93.78	96.99	51.10	74.75	73.47	93.31	80.56
NN	AUC	91.06	94.14	90.69	82.72	76.31	91.58	87.75
	AP	96.36	96.50	86.51	85.94	79.88	92.83	89.67
Variation	AUC	91.32	93.45	91.13	77.06	73.53	81.76	84.70
	AP	96.18	95.47	86.37	83.33	77.11	81.06	86.58

Table 4: Anomaly detection results for the MVTec dataset.

Methods	Metrics	Bottle	Cable	Capsule	Hazelnut	Metal Nut	Pill	Toothbrush	Transistor	Mean
Proposed	AUC	99.71	87.73	86.39	95.87	79.28	86.74	100.0	93.06	**91.09**
	AP	99.90	92.54	96.71	97.90	94.88	97.23	100.0	91.68	**96.35**
AE (L_2)	AUC	89.77	82.70	54.89	85.23	59.45	79.85	76.68	86.35	75.31
	AP	96.83	89.70	87.12	91.74	87.36	95.59	91.03	85.72	91.39
Deep Feature	AUC	96.71	83.61	88.37	90.29	68.93	71.71	91.67	85.33	83.27
	AP	98.90	90.45	96.40	95.01	90.21	92.38	96.85	85.51	93.89
NN	AUC	81.02	81.30	69.78	52.83	60.16	63.66	95.84	81.12	68.12
	AP	93.78	88.11	91.09	74.29	87.76	88.71	98.46	78.64	87.29
Variation	AUC	79.25	68.20	46.05	49.13	42.95	62.86	86.48	73.09	58.07
	AP	93.12	77.88	83.08	70.93	79.20	87.56	94.36	75.15	81.96
GeoTrans	AUC	74.4	78.3	67.0	63.0	35.9	63.0	97.2	86.9	63.60
	AP	*	*	*	*	*	*	*	*	*
GANomaly	AUC	89.2	75.7	73.2	74.3	78.5	74.3	65.3	79.2	77.53
	AP	*	*	*	*	*	*	*	*	*
VAE	AUC	89.7	65.4	52.6	87.8	57.6	76.9	69.3	62.6	71.66
	AP	*	*	*	*	*	*	*	*	*
AnoGAN	AUC	62.0	38.3	30.6	69.8	32.0	77.6	74.9	54.9	51.71
	AP	*	*	*	*	*	*	*	*	*
AE (SSIM)	AUC	83.4	47.8	86.0	91.6	60.3	83.0	78.4	72.5	75.35
	AP	*	*	*	*	*	*	*	*	*

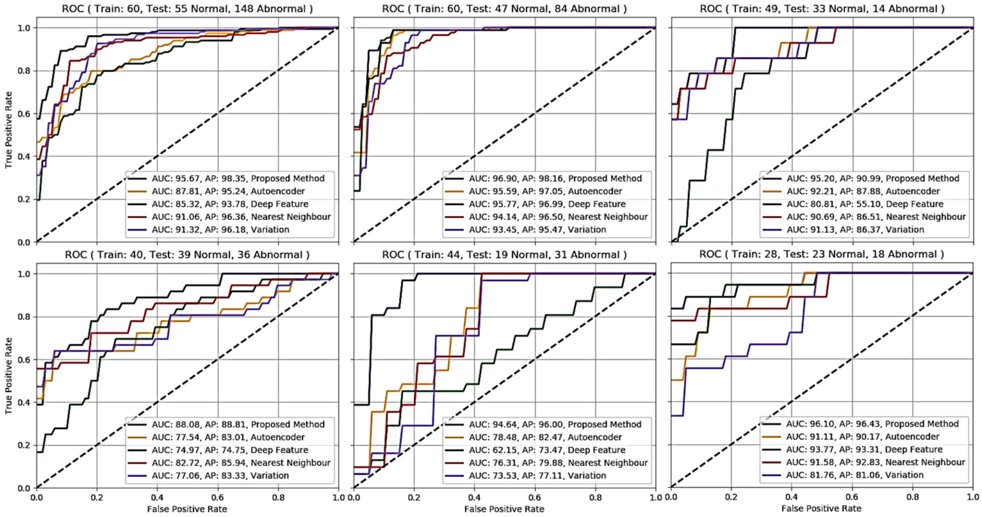

Figure 7: Comparison of ROC curves obtained for different methods and datasets, (top row, left to right): sets #1-3, (bottom row, left to right): sets #4-6 of zipper cursor dataset.

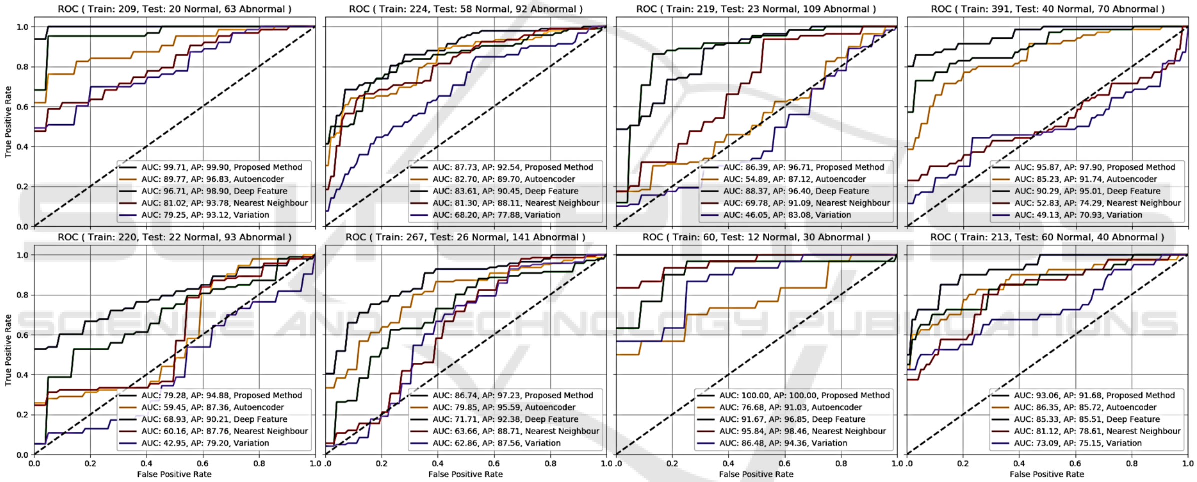

Figure 8: Comparison of ROC curves obtained for different methods and datasets, (top row, left to right): Bottle, Cable, Capsule, Hazelnut, (bottom row, left to right): Metal Nut, Pill, Toothbrush, Transistor of MVTec dataset.

For the zipper cursor dataset where there are not enough samples for training, e.g. sets #4-6, the performance of the proposed method along with other approaches decline. For the MVTec dataset, good performance can be observed on the “bottle”, “toothbrush”, “hazelnut”, and “transistor”, while it yields comparably poorer results for “metal nut”, “cable”, and “pill”. This is because the latter objects contain certain random variations on the objects’ surfaces, which prevents the model from learning detailed information for most of the image pixels.

For the final experiment, we demonstrate the reconstructed images and anomaly maps generated using the proposed CPCAE method for some samples of zipper cursor shown in Figure 9, and MVTec datasets illustrated in Figure 10. For the zipper cursor dataset, anomalies manifest themselves in the different types of defects such as bubble, residue, scratch, and halo as shown in Figure 9 (b), and for the MVTec dataset, anomalies are consisting of broken, crack, cut, color, contamination, and misplaced as illustrated in Figure 10 (b). It can be seen from the results that the proposed method fails to reconstruct the defected regions, while it can generalize well to reconstruct the normal unseen images within normal specification ranges.

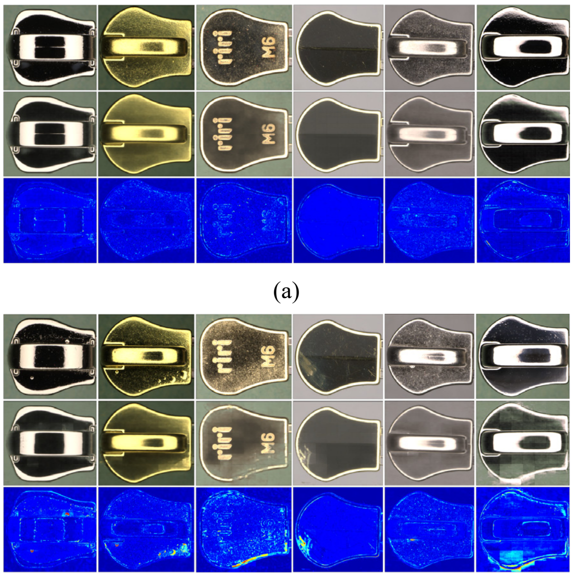

Figure 9: Anomaly detection results for (a) normal and (b) defected samples, top to bottom: input image, reconstructed image using AE, and anomaly map; left to right, sets #1 to #6 of zipper cursor dataset.

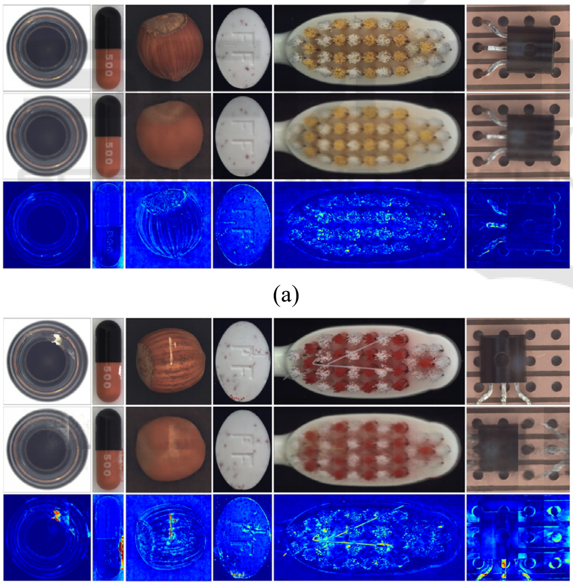

Figure 10: Anomaly detection results for (a) normal and (b) defected samples, top to bottom: input image, reconstructed image using AE, and anomaly map; left to right, "Bottle", "Capsule", "Hazelnut", "Pill", "Toothbrush" and "Transistor" of MVTec dataset.

5 CONCLUSIONS AND FUTURE WORKS

A novel framework for the semi-supervised anomaly detection tasks is proposed here to introduce a method for zipper cursors' visual inspection. The proposed method uses a conditional path-based convolutional autoencoder to tackle the challenges related to the high-resolution images in industrial inspection scenarios. In addition, we use a binary classification on top of the autoencoder result to leverage the transfer learning through feature extraction via a pre-trained CNN network and to avoid computing anomaly scores using the simple per-pixel comparisons of autoencoder. We demonstrate state-of-the-art performance on different datasets, including the zipper cursor dataset and the recently introduced MVTec dataset.

For future work, we investigate other types of deep learning frameworks, e.g. variational autoencoder and generative adversarial network instead of autoencoder applied in the proposed method. In addition, regarding deep feature one-class classification, we would like to explore different one-class classifiers to improve the results.

ACKNOWLEDGEMENTS

This work has been supported by the Swiss Innovation Agency (Innosuisse) project 27371.1 IP-ICT. The authors would like to thank RIRI SA for their assistance in preparing zipper cursor datasets and their valuable feedback.

REFERENCES

Akcay, S., Atapour-Abarghouei, A., and Breckon, T. P. (2018). GANomaly: Semi-Supervised Anomaly Detection via Adversarial Training. In *ACCV*.

Andrews, J.T.A., Tanay, T., Morton, E.J., and Griffin, L.D. (2016). Transfer Representation Learning for Anomaly Detection. In *Anomaly Detection Workshop at ICML*.

Badrinarayanan V., Kendall A. and Cipolla R. (2017). SegNet: A Deep Convolutional Encoder-Decoder Architecture for Image Segmentation. *IEEE Transactions on Pattern Analysis and Machine Intelligence*, 39 (12): 2481-2495.

Baklouti, R., Mansouri, M., Nounou, M., Nounou, H., and Hamida, A.B. (2016). Iterated robust kernel fuzzy principal component analysis and application to fault detection. *Journal of Computational Science* 15: 34–49

Bergman, L., Cohen, N., and Hoshen, Y. (2020). Deep Nearest Neighbor Anomaly Detection. ArXiv, abs/2002.10445.

Bergmann, P., Fauser, M., Sattlegger, D., and Steger, C. (2019a). MVTec AD - A Comprehensive Real-World Dataset for Unsupervised Anomaly Detection. IEEE Conference on Computer Vision and Pattern Recognition (CVPR), pages 9592-9600.

Bergmann, P., Fauser, M., Sattlegger, D., and Steger, C. (2020). Uninformed students: Student-teacher anomaly detection with discriminative latent embeddings. In *CVPR.*

Bergmann, P., Lowe, S., Fauser, M., Sattlegger, D., and Steger, C. (2019b). Improving Unsupervised Defect Segmentation by Applying Structural Similarity to Autoencoders. In *Proceedings of the 14th International Joint Conference on Computer Vision, Imaging and Computer Graphics Theory and Applications*, volume 5, pages 372–380

Breunig, M., Kriegel, H., Ng, R.T., Sander, J. (2000). LOF: identifying density-based local outliers. *International Conference on Management of Data (SIGMOD)*, pages 93-104

Burlina, P., Joshi, N., and Wang, I. (2019). Where's Wally Now? Deep Generative and Discriminative Embeddings for Novelty Detection. *IEEE Conference on Computer Vision and Pattern Recognition (CVPR)*, pages 11507-11516

Chang, S., Du, B., and Zhang, L., (2019). A Sparse Autoencoder Based Hyperspectral Anomaly Detection Algorithm Using Residual of Reconstruction Error. *IEEE International Geoscience and Remote Sensing Symposium*, pages 5488-5491

Chao-Qing, H., et al. (2019). Inverse-Transform AutoEncoder for Anomaly Detection." ArXiv abs/1911.10676.

Chollet, F. (2017). Xception: Deep Learning with Depthwise Separable Convolutions. *IEEE Conference on Computer Vision and Pattern Recognition (CVPR)*, pages 1800-1807

Davis, J., and Goadrich, M. (2006). The relationship between precision recall and ROC curves. *In International Conference on Machine Learning (ICML)*, pages 233–240

Deng, J. et al. (2009). Imagenet: A large-scale hierarchical image database. *IEEE Conference on Computer Vision and Pattern Recognition CVPR*. pages 248–255.

Eskin, E. (2000). Anomaly detection over noisy data using learned probability distributions. In *Proceedings of the 17th International Conference on Machine Learning*, pages 255-262.

Golan, I., and El-Yaniv, R. (2018). Deep anomaly detection using geometric transformations. In *NeurIPS.*

Guo, J., Liu, G., Zuo, Y. and Wu, J. (2018). An Anomaly Detection Framework Based on Autoencoder and Nearest Neighbor. *15th International Conference on Service Systems and Service Management (ICSSSM)*, pages 1-6

Harrou, F., Kadri, F., Chaabane, S., Tahon, C., Sun, Y. (2015). Improved principal component analysis for anomaly detection: Application to an emergency department. *Computers & Industrial Engineering* 88: 63–77

Jinwon, An., and Sungzoon, Cho. (2015). Variational Autoencoder based Anomaly Detection using Reconstruction Probability. *SNU Data Mining Center, Tech. Rep. Special Lecture on IE* 2:1–18

Kawachi, Y., Koizumi, Y., and Harada, N. (2018). Complementary set variational autoencoder for supervised anomaly detection. *IEEE International Conference on Acoustics, Speech and Signal Processing (ICASSP)*, pages 2366–2370.

Kingma, D. P., Welling, M. (2014). Auto-Encoding Variational Bayes. *International Conference on Learning Representations (ICLR)*, pages 1-14

Kornblith, S., Shlens, J., and Le, Q. V. (2019). Do better imagenet models transfer better? *IEEE Conference on Computer Vision and Pattern Recognition (CVPR)*, pages 2661-2671.

Krizhevsky, A., and Hinton, G. (2009). *Learning multiple layers of features from tiny images*. Technical Report. University of Toronto.

LeCun, Y. (1998). The mnist database of handwritten digits. http://yann. lecun. com/exdb/mnist/

Matsubara, T., Hama, K., Tachibana, R., and Uehara, K. (2018). Deep generative model using unregularized score for anomaly detection with heterogeneous complexity. arXiv preprint arXiv:1807.05800.

Nalisnick, E., Matsukawa, A., Whye The, Y., Gorur, D., and Lakshminarayanan, B. (2018). Do Deep Generative Models Know What They Don't Know? *arXiv preprint arXiv:1810.09136*.

Napoletano, P., Piccoli, F., and Schettini, R. (2018). Anomaly Detection in Nanofibrous Materials by CNN-Based Self-Similarity. *Sensors*, 18 (1): 209

Nazaré, S. et al. (2018). Are pre-trained CNNs good feature extractors for anomaly detection in surveillance videos?" *ArXiv abs/1811.08495*.

Olive, D.J. (2017). Principal Component Analysis, *Robust Multivariate Analysis*, Springer: 189–217.

Oza, P. and Patel, V. M. (2019). One-Class Convolutional Neural Network. IEEE Signal Processing Letters, 26 (2): 277-281.

Perera, P., and Patel, V. M., (2019). Learning Deep Features for One-Class Classification. IEEE Transactions on Image Processing, 28 (11): 5450-5463.

Pol, A., Berger, V., Germain, C., Cerminara, G., and Pierini, M., (2019). Anomaly Detection with Conditional Variational Autoencoders. *IEEE International Conference On Machine Learning and Applications (ICMLA)*, pages 1651-1657

Ribeiro, M., Lazzaretti, A. E., and Lopes, H. S. (2018). A study of deep convolutional auto-encoders for anomaly detection in videos. *Pattern Recognition Letters*, 105: 13-22,

Ruff, L., Görnitz, N., Deecke, L., Siddiqui, S., Vandermeulen, R.A., Binder, A., Müller, E., and Kloft, M. (2018). Deep One-Class Classification. In *Proceedings of the 35th International Conference on Machine Learning*, volume 80, pages 4393-4402

Saeedi, J., Dotta, M., Galli, A. et al. (2021). Measurement and inspection of electrical discharge machined steel surfaces using deep neural networks. *Machine Vision and Applications* 32, 21: 1-15

Schlegl, T., Seebock, P., Waldstein, S. M., Erfurth, U. S., and Langs, G. (2017). Unsupervised Anomaly Detection with Generative Adversarial Networks to Guide Marker Discovery. In *International Conference on Information Processing in Medical Imaging*, pages 146–157.

Scholkopf, B., Platt, J.C., Shawe-Taylor, J.C., A.J. Smola, and R.C. Williamson. (2001). Estimating the support of a high-dimensional distribution. *Neural Computing*, 13(7): 1443–1471.

Steger, C., Ulrich, M., and Wiedemann, C. (2018). *Machine Vision Algorithms and Applications*. Wiley-VCH, Weinheim, 2nd edition.

Szegedy, C., Vanhoucke, V., Ioffe, S., et al. (2016). Rethinking the Inception Architecture for Computer Vision. In *Proceedings of the IEEE Computer Society Conference on Computer Vision and Pattern Recognition*, pages 2818–2826

Tang, B., He, H. (2017). A local density-based approach for outlier detection, *Neurocomputing*, 241: 171–180

Tax, D.M.J., and Duin, R.P.W. (2004). Support vector data description. *Mach. Learn*., 54(1): 45–66.

Vaikundam, S., Hung, T., and Chia, L.T. (2016). Anomaly region detection and localization in metal surface inspection. *IEEE International Conference on Image Processing (ICIP)*, pages 759-763

Van der Maaten, L. and Hinton, G. E. (2008). Visualizing high-dimensional data using t-SNE. *Journal of Machine Learning Research* 9:2579–2605

Xiao, H., Rasul, K., and Vollgraf, R. (2017). Fashion-mnist: a novel image dataset for benchmarking machine learning algorithms. arXiv preprint arXiv:1708.07747.

Xu, H., Caramanis, C., and Sanghavi, S. (2012). Robust PCA via outlier pursuit. *IEEE Transactions on Information Theory*, 58 (5): 3047-3064

Yildirim, O., Tan, R.S., Acharya, U. R., (2018). An efficient compression of ECG signals using deep convolutional autoencoders, *Cognitive Systems Research*, volume 52, pages 198-211